8. DIAGNOSIS OF TURBIDITES AT SITES 386 AND 387 BY PARTICLE-COUNTER SIZE ANALYSIS OF THE SILT (2-40 μm) FRACTION

I. N. McCave, School of Environmental Sciences, University of East Anglia, Norwich, England

ABSTRACT

A new method of processing data from a Model T Coulter Counter which allows construction of frequency curves based on 41 points at 1/9-φ intervals is described. The method is applied to samples from Paleocene and Eocene presumed siliceous turbidites and reveals (1) upward fining of coarse size modes, (2) upward increase of fine modes and, (3) evidence of basal erosion in the incorporation of fine modes from underlying pelagic sediment into the basal part of a turbidite. Subsequent analysis of samples from units for which a turbidite origin was in doubt reveals that most of these too are turbidites.

INTRODUCTION

At Site 386 starting in Core 4, beds of silt with up to 10 per cent fine sand occur. They are overlain by sometimes thick (>1 m) sequences of silty clay and clayey silt showing some upward gradation in properties (e.g., laminated → homogeneous → burrow mottled) but no obvious size grading above the basal silt. Preliminary grain size analysis of part of the silt fraction of samples from some beds in Units 4A at Site 386 and 3A at Site 387 (Figure 1) showed a progressive shift in position of modes to finer sizes with height above the base of a bed. A wider suite of samples was taken to see whether grading could be detected in other units where a turbidite origin was (or in cases was *not*) suspected.

Presumed Turbidites

The beds initially believed to be turbidites in lithologic Units 4A (386) and 3A (387) show a characteristic set of subdivisions denoted by the greek letters α to ϵ (Table 1). Grain size analyses averaged for the various subdivisions given in this table show the graded nature of the deposits. The lowermost α and β divisions correspond to the A and B intervals of the classic Bouma sequence (Bouma, 1962). γ and δ are essentially the same with δ having post-depositional burrow mottles. This γ division material forms the bulk of most of these turbidites. It is structureless and must be seen as the product of fairly rapid deposition of the fine material (silty clay) forming the bulk of the turbidity current. If deposition had been slow then some sorting, lamination, and/or structures would be expected. Drilling disturbance is not responsible for the homogeneity of the γ layers. Whereas the γ and δ division material is light green and calcareous (average 22% $CaCO_3$ in γ), ϵ layers are essentially non-calcareous (<2%) and dark green in color. The latter are thought to be the product of pelagic deposition below the carbonate compensation depth. Van der Lingen (1969) has proposed that

this should be termed the F division in a modified Bouma sequence, retaining the E of the original proposal (Bouma, 1962) for material deposited from the tail of a turbidity current (see also Hesse [1975] on this subject).

Possible Turbidites

The lithologic units containing beds of possible turbidite origin are 3A, 4C, 4D, and 6 at Site 386 and 3B at Site 387.

Site 386, Unit 3A

This contains at most a dozen turbidites with good graded sands. The point in doubt is whether thick sections (up to 1 m in thickness) overlying the graded sands are also graded in some way and are also of turbidite origin. The turbidite sands do contain some carbonate whereas some determinations on the material between the sands shows zero carbonate, so it may be pelagic in origin.

Site 386, Unit 4C

The cherty claystones of this unit are partly irregular interbeds of greenish gray claystone and chert and partly regular sequences. The regular sequences comprise a basal greenish gray to olive-gray faintly laminated part (β in higher Units 4A and 4B), a dark greenish gray homogeneous part (γ), and a mottled cherty top (ϵ maybe with δ). These sequences average 35 to 50 cm in thickness. The occurrence of the chert at the β/ϵ part of the sequence suggests possible reaction between the basal part of a unit more rich in siliceous debris with pelagic sediment more rich in clay. It is possible that these sequences represent some sort of productivity-related cycle rather than turbidites, so some analyses have been made of them.

Site 386, Unit 4D

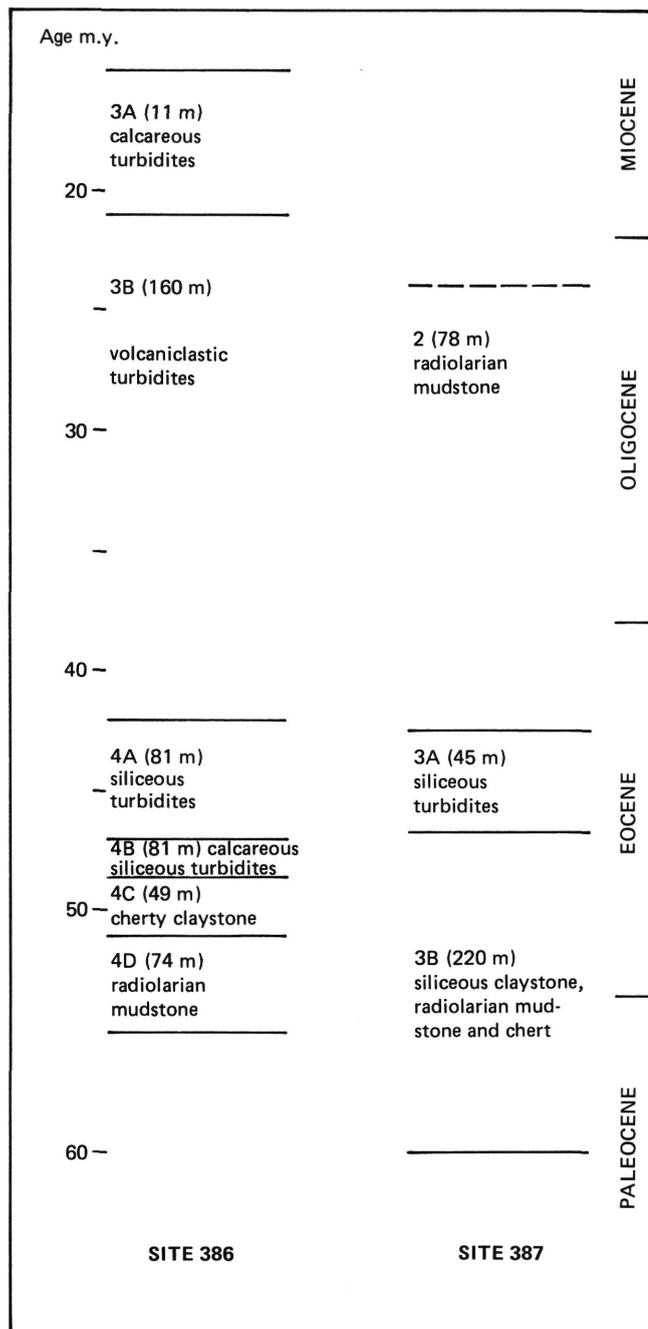This unit contains a number of $\beta\gamma\epsilon$ cycles with cherty divisions similar to those of Unit 4C. Cycle

Figure 1. *Correlation of the Paleogene units at Sites 386 and 387.*

TABLE 1
Turbidites of Units 4A (Site 386) and 3A (Site 387)

Layer[a]	Characteristics	Interpretation	Sand	Silt[b]	Clay
α	Base of next unit				
ϵ	Dark green non-calcareous claystone	Pelagic inter-turbidite deposit below CCD			
δ	Light green calcareous silty claystone with dark green burrow mottles	Sediment burrowed down into calcareous material	0	30	70
γ	Light green calcareous silty clay-stones	Fine sediment bulk of current deposited rapidly	0	30	70
β	Laminated to faintly laminated silty claystone	Plane bed deposition in upper flow regime	1	44	55
α/β	Boundary—gradational		3	54	43
α	Massive to graded clayey siltstone to sandy siltstone	Rapid deposition in upper flow regime	13	67	20

[a] α and β are equivalent to Bouma's (1962) A and B divisions, γ and δ to his E division (less certainly), and ϵ to the F division of Van der Lingen (1969).
[b] Silt = 63 μm to 3.9 μm (4 to 8 $\emptyset$). Size data from the DSDP laboratory at Scripps Institution of Oceanography.

thickness is mainly from 50 to 60 cm. In the upper part of the unit (Core 32) the cycles are simply $\gamma\epsilon$ repeated, with ϵ being cherty. These too are possibly turbidites, or perhaps the product of some productivity-related mechanism.

Site 387, Unit 3B

There are a number of different cycle types in this unit. Cores 13 to 18, 22, and 23 contain $\beta\gamma\epsilon$ layers with considerable silicification throughout and chert or porcellanite in the ϵ layer. Cores 19 to 21 and 27 contain units similar to the above with the addition of a graded α layer. In Core 20 there is some nannofossil claystone. Cores 24 to 26 contain repeated 20- to 30-cm-thick units of ABAB type where A is olive-black, organic-carbon-rich (>1% C), partly laminated, slightly burrow mottled claystone, and B is intensely mottled dark greenish gray claystone. The burrowing and organic carbon makes these look unlike turbidites and more like repeated oxygen-depletion/carbon-input events. The question about the $\beta\gamma\epsilon$ cycles here is the same as in Units 4C and 4D at Site 386.

Site 386, Unit 6

The greenish gray and black claystones contain a large number of homogeneous beds with a layer a few millimeters thick of mud clasts at the base. The lack of burrowing suggests rapid deposition of the bed, but apart from this and the mud clasts there is no evidence from grading or structures that these might be turbidites. A test was made on these units.

METHODS

General

The analyses were made with a Model T Coulter Counter using a new method giving 41 data points in the range 1.71 μm to 40.3 μm at a 1/9 ϕ spacing. Small samples of a gram or less were selected on the ship or in the core repository. They were selected on the basis of position in a supposed turbidite, and care was taken

to avoid contamination by taking apparently homogeneous pieces of sediment and then scraping their surface off and discarding the scrapings.

Sample Treatment

Samples were prepared for analysis by scraping material into a beaker of freshly filtered (through a 0.4 μm Nuclepore filter) saline (1%) solution with nonidet, a detergent-type dispersant. The suspension was usually allowed to soak for a minute or two before a first treatment of 10-15 seconds in an ultrasonic bath at 45 kHz frequency. The suspension was then examined and if any aggregates could be seen the treatment was repeated. Unconsolidated materials (uncemented) tended to disperse rapidly. The suspension was poured through a 63 μm sieve, stirred vigorously, and an aliquot was decanted into the beaker for counting. Prior to counting this was further diluted to give a concentration level acceptably low so as to avoid severe coincidence problems (Sheldon and Parsons [1967] detail methods and problems for earlier types of Coulter Counter including coincidence).

The Coulter Counter

The Model T Coulter Counter has 15 channels (numbered 0 to 14) to which pulses proportional to particle volume generated by the passage of particles through an orifice are assigned and counted. Each channel is assigned particles of mean volume twice that of the next lower channel, the coarse-size end being channel 0. The machine can count particles of diameter from about 2 to 40 per cent of the diameter of the orifice. The orifice used for this work was 100 μm, giving a size range of 2 to 40 μm for these determinations. Channel 0 which accumulates counts of all particles coarser than the 0/1 channel-size edge was ignored. A constant check was kept on blank levels, an average blank being kept up to date and a correction applied to the counts.

The doubling of volume succession gives a 1/3-ϕ interval ($\phi = -\log_2 d$ [mm] where d is grain diameter); diameter doubles every 3 channels. Particle volume can be obtained from number of particles counted if it is assumed that one particle in channel 0 has a volume of one unit or 2^0. Then in channel 1, 2^1 particles makes up one unit, in channel 4, 2^4 particles make up one unit, and so on. The meaning of these volume units can be ascertained through calibration experiments with material of known size. The calibration may be changed with an attenuation control whose value A figures in the relationship

$$K = d(2^w/A)^{1/3}$$

where K is the aperture constant determined by calibration experiments, d is grain diameter in micrometers corresponding to the boundary between channel w and the next smaller size channel. Thus for our 100 μm aperture tube with $K = 5.51$, we find that a setting of

$A = 392$ results in the size edge between channels 1 and 2 being 32 μm.

The 41 Point Distribution

The system for obtaining 41 points rather than 14 is outlined in Figure 2. It depends on making three size determinations on a given sample, each one with a different attenuation setting adjusted so that there is one third overlap of channels. In Figure 2 X, Y, and Z denote numbers of particles counted in the channels given by the subscript number. By adding up the X, Y, and Z values in the way shown, a first approximation to the 41 point distribution may be obtained. The sizes progress in 1/9 interval powers of two. To convert the $(X + Y + Z)$ sums of particle number to volume they must be divided by an appropriate number. In this case the progression 2^0, $2^{1/3}$, $2^{2/3}$, etc. was used for size ranges 1 to 41. (Note: with a 1/3 ϕ progression particle number is divided by 2^0, 2^1, 2^2, etc., so for a 1/9 ϕ progression 2^0, $2^{1/3}$, $2^{2/3}$ is necessary.)

However, this simple addition, which for example uses the number X_2 three times in size ranges 4, 5, and 6, assumes that the particles are equally distributed across channel 2. This is obviously not the case, so the next stage is to redistribute the particle count X_2 across the channel. Denoting the sums in Figure 2 by T, e.g., $T_4^{n=0} = (X_2 + Y_1 + Z_1)$, $T_5^{n=0} = {}_L(X_2 + Y_1 + Z_1)$, etc. then a revised value for T_4 given by

$$T_4^{n=1} = 3\left[X_2 \cdot \frac{T_4}{(T_4 + T_5 + T_6)} + Y_1 \cdot \frac{T_4}{(T_2 + T_3 + T_4)} + Z_1 \cdot \frac{T_4}{(T_3 + T_4 + T_5)} \right]$$

takes into account the gradient of particle number as determined by the initial ($n = 0$) addition of particle number. In this the group

$$3\left[X_2 \cdot \frac{T_4}{(T_4 + T_5 + T_6)} \right] = X_2^{n=1}$$

and similarly the other groups are $Y_1^{n=1}$ and $Z_1^{n=1}$. The process may now be repeated and $T_4^{n=2}$ is obtained using $X_2^{n=1}$, $Y_1^{n=1}$, $Z_1^{n=1}$ and $T_3^{n=1}$, $T_4^{n=1}$, etc. It was found that visually acceptable results were produced with five iterations ($n=5$) and a gentle smoothing. This data "massaging" iteration loop was devised and programmed by my colleague Dr. C. E. Vincent. The particle volumes for the 41 size ranges so produced were expressed as a percentage of the 1.71 to 40.3 μm size fraction.

The Mcϕ Scale

When working in the silt range, it is most convenient to deal with sizes in micrometers expressed as powers of 2. Thus the scale 1, 2, 3, 4 is 2^1, 2^2, 2^3, 2^4
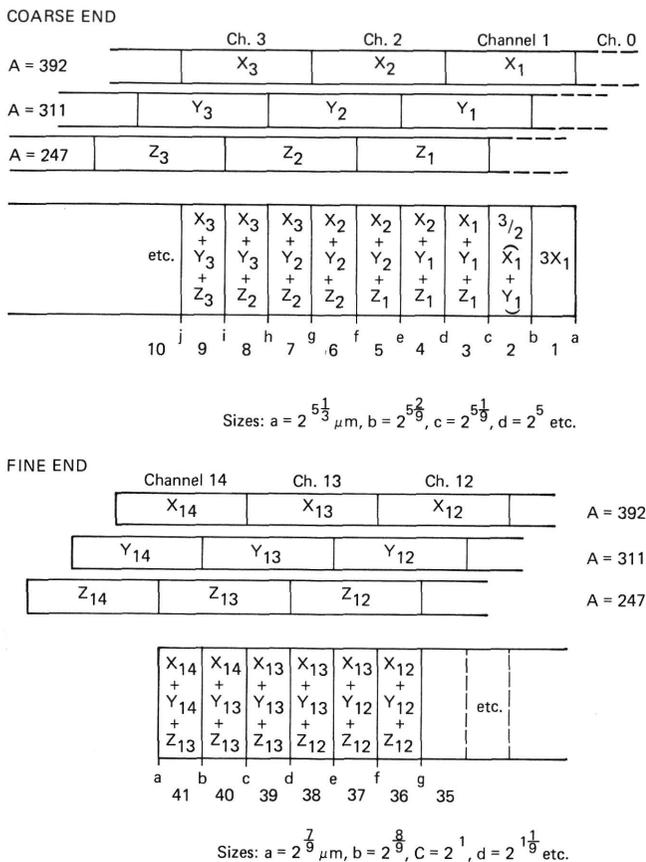
Figure 2. *The scheme for addition of particle number counts to yield a 41 point distribution.* $X_1, X_2 \ldots,$ $Y_1, Y_2 \ldots, Z_1, Z_2 \ldots,$ etc., *denote the number of counts in the channel indicated by subscript number. A is the setting of the attenuation control. Note the end-effects for size ranges 1 and 2 and 40 and 41. The coarse end uses only one and two runs while the fine end uses channel 14 for 40 and 41.*

Figure 3. *Examples of analyses of the same sample to demonstrate reproducibility. Number 1 has the data points shown; all the other curves here and in Figures 4 to 10 are based on the same number of points; note the end effect on the points ringed with a dashed line. Subsample 1, a one-off analysis of a single scraping; 2A and 2B, 3A and 3B are replicate analyses of two separate scrapings. The major mode maintains its position at 1.6 to 1.75 Mcφ and another mode at 3.1 to 3.2 Mcφ is constant in all these analyses.*

μm or 2, 4, 8, 16 μm, etc. The intervals in this scale are ϕ intervals, being based on 2, but the numbers are not ϕ units. I therefore suggest the Scottish form Mcϕ, loosely meaning "son of phi," indicating the derivative nature of the scale. The diagrams are labeled with scales in μm and Mcϕ.

Problems

The principal difficulties associated with counter analysis of fine sediments are in sampling and reproducibility of results and in flocculation.

Sampling and reproducibility are closely related because the amount of material needed for the analysis is generally a few milligrams. It is simpler and easier to select an apparently homogeneous and representative subsample for analysis by scraping the sample than it is to disperse the whole sample and then go through a large number of wet splitting operations.

The reproducibility of the method may be gauged by reference to Figure 3, in which an original one-shot run is shown together with two other duplicate subsamples. The main features of the distribution are reproduced in each case.
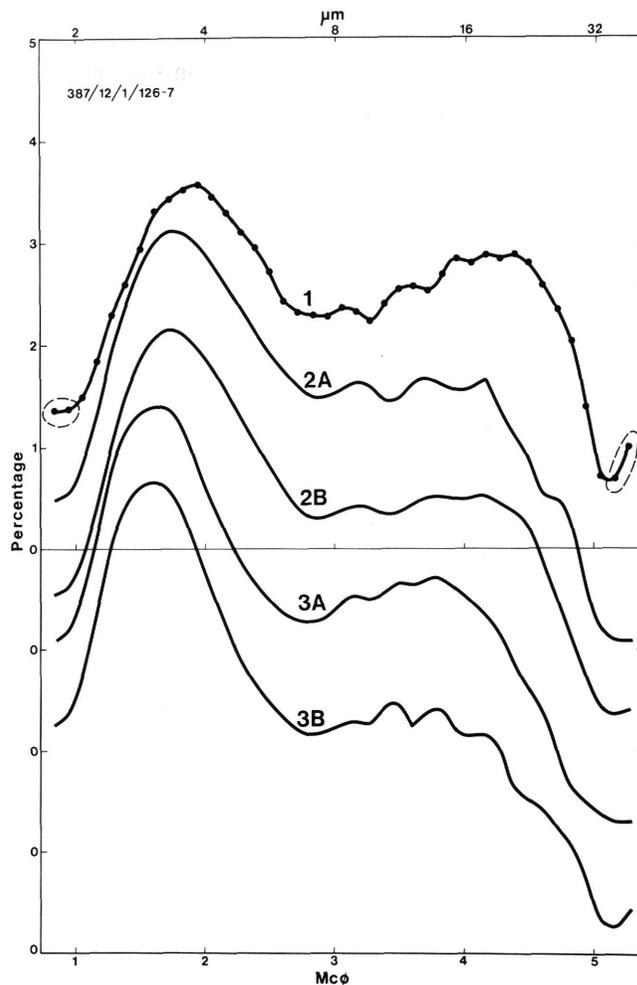
Flocculation of the sample during counting is very occasionally a problem. It usually occurs when most of the sample is clay (<2 μm) and the silt fraction being counted is a small proportion of the whole. The problem can partially be cured by using calgon as a dispersant and by not stirring the suspension during counting. However one is not sure that this is completely successful.

Comments

The procedure for generating multipoint distributions was devised and adopted because the modal composition of sediments is best seen using frequency curves. A $1/9\phi$ interval histogram is close enough to a frequency curve to be considered as such. This, the differentiated form of the cumulative curve, is far more informative visually, particularly if the cumulative curve is one of log (particle number) versus grain size.

The frequency plots presented here allow one to make correlations based on the overall size of the sample in the silt range as well as on particular modes and shifts in modal position.

RESULTS AND DISCUSSION

The results are presented in graphical form with the individual size frequency curves superimposed in stratigraphical order for each unit (Figures 4 through 10). The characteristics of curves from undisputed turbidites at Sites 386 and 387 are discussed first, then the problematical units are examined.

Turbidites at Site 386, Unit 4A and Site 387, Unit 3A

Results: Five turbidites from these units have been analyzed with results shown in Figures 4 and 5. The principal features shown by these diagrams are: (a) an upward shift toward finer sizes of the coarse mode (see 387-10-6, CC and 387-12-1); (b) an upward growth in the proportion of the sample in a fine mode (1.25 to 2.75 Mcϕ) (see 386-15-2,3, α to γ layers; 386-15-1,2 growth within γ layer; 387-10-6, CC, growth from γ to δ layers); and (c) indication of basal erosion during emplacement by (i) a fine mode (centered around 2 Mcϕ) in the basal (α) sample matching a corresponding mode in the underlying (ϵ) sample (see 387-10-6, CC and 387-12-1) and (ii), overall finer basal sample lacking coarse mode peak (see 386-15-2,3 and 387-9-3).

Discussion: The features described under point c are thought to demonstrate incorporation of ϵ material in the basal part of a turbidite. This together with the evidence of fining/grading of points a and b provide an elegant set of grain size criteria for the diagnosis of turbidites. The existence of a finer basal layer is not always indicative of basal erosion as Middleton (1967) detected reverse grading in some basal samples from experimental turbidites. However the matching of modes was also used by Middleton to distinguish between genuine reverse grading and basal erosion. In the present case reverse grading does not seem to be the feature observed; basal erosion of underlying material is most likely.

Thus it is surprising that the finer sample at 63-64 cm in 386-15-3 does not show the coarse mode at 4.9 Mcϕ displayed by the underlying ϵ layer. This could be because of diagenetic changes in the ϵ layer. Samples from deeper at Sites 386 and 387 showed much development of porcellanite in the ϵ layers. However all the ϵ layers in this group of samples disaggregated readily and most of them show more material in coarse modes (4-5 Mcϕ) than underlying δ and γ layers, so this may be an original feature of the sediment.

Possible Turbidites: Site 386, Unit 4C (Figure 6)

Results: The data from this site are poor because of disaggregation problems. Of the sequence in 386-29-2, samples at 111 and 128 disaggregated with difficulty and probably not completely, sample 105 was partly
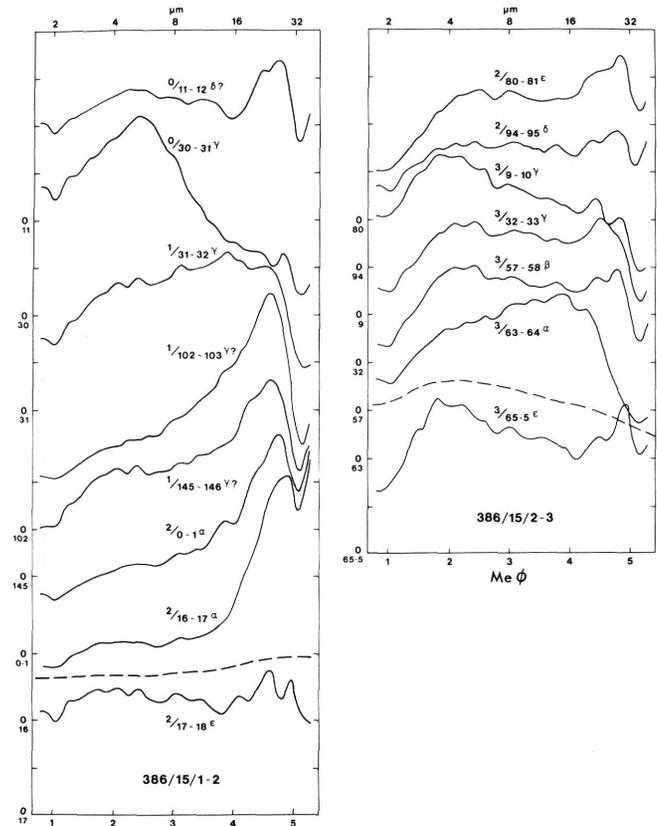

Figure 4. *Analyses of samples from Unit 4A, Site 386. The dashed line marks the boundary at the base of a turbidite.*

porcellanite and a sample at 136 cm was rock. Similar problems afflicted the upper two samples in 386-30-1,2 and no conclusions can be based on this either.

Discussion: The samples from 386-38-4 might be from a turbidite, but there are too few to be sure. The lower β has a pronounced fine mode possibly picked up by erosion, the upper β has both coarse and fine modes while the overlying γ has pronounced growth of the fine mode. The sizes in the 58-59 cm sample are probably spurious because of porcellanization. In conclusion Unit 4C might contain turbidites but the evidence is obscured by diagenetic change (however, see below the results for the coeval Unit 3B at Site 387 and preceding Unit 4D at Site 386).

Site 386, Unit 4D (Figure 7)

Results: 386-34-2 resembles 386-15-2,3 in growth of the fine mode upwards and in the basal sample lacking the coarsest mode but appearing and declining higher up. The unit system is hard to apply here but 147 is a β, 127 and 105 are β/γ (?), 64 is γ, and 42 is δ/ϵ (?). Sequence 386-32-3 also shows the fine mode in the basal sample (base of the unit is at 45.5 cm) together with some coarse material, then growth of the fine mode from 30 through 17 to 10 cm samples.

Discussion: The two sequences from this subunit display most of the features found in the accepted turbidites higher up and an origin by deposition from turbidity currents is most likely.
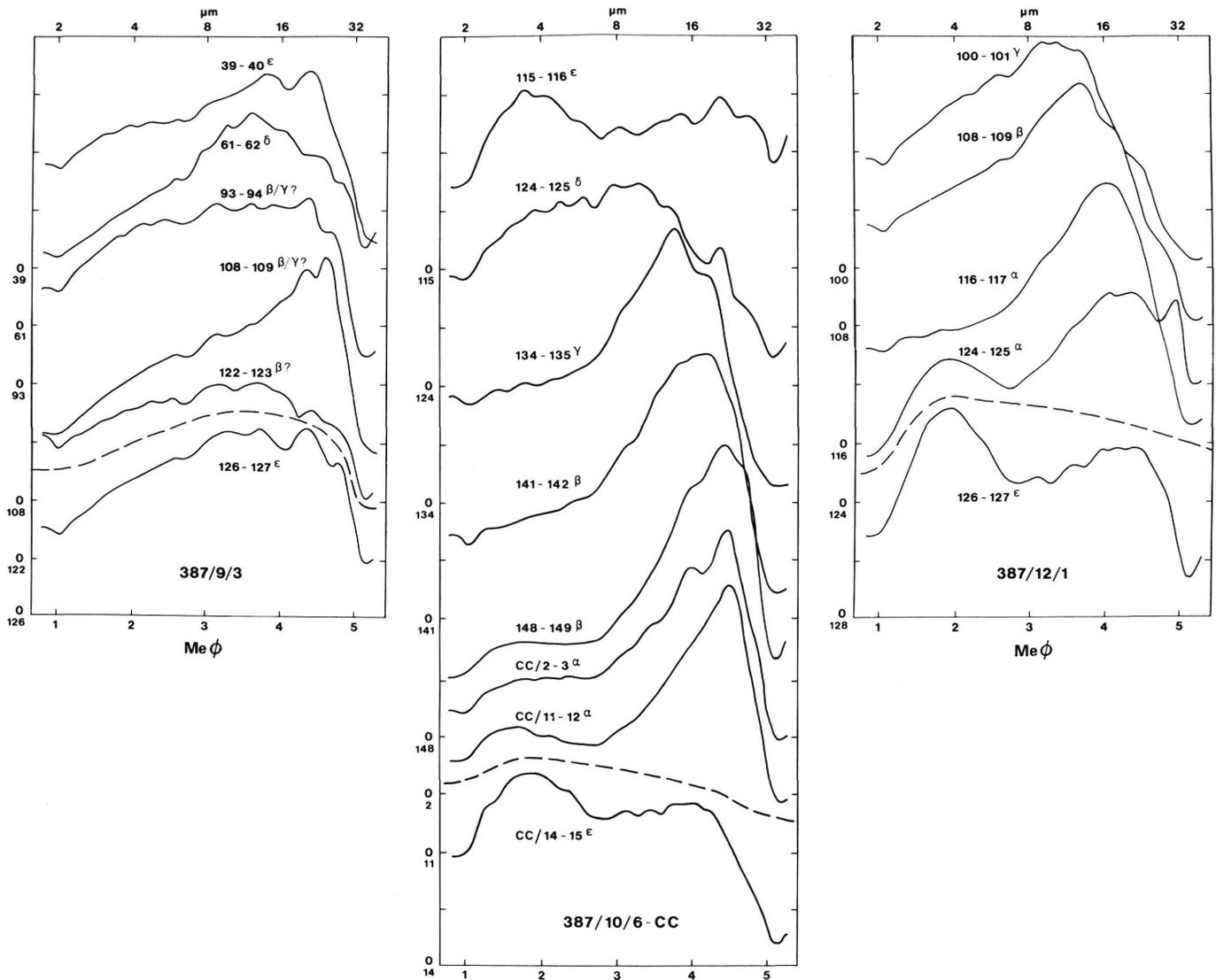
Figure 5. *Analyses of samples from Unit 3A, Site 387. The dashed line marks the boundary at the base of a turbidite.*

Site 387, Unit 3B (Figure 8)

Results: The sequence in 387-19-3 shows a decline in the coarse mode (most of which appears to be >40 μm) and a progressive growth of the fine mode. The base of the sequence is at 101 cm so the characteristics of the sample at 100-101, even if incompletely disaggregated, show more fine mode than the higher α sample, presumably a result of basal erosion. The α layer of 387-27-1 also has much material >40 μm in size, but in the α-β-γ sequence the progressive shift of the coarse mode to finer sizes can be seen.

The sample at 40 cm takes a small jump to coarser sizes and is then succeeded by a finer ϵ. The γ sample at 75 cm comes from a homogeneous brownish black (5YR 2/1) claystone whereas the β at 40 cm is a diffusely laminated dark greenish gray (5 GY 4/1) claystone. The α samples at 52 and 100 are from greenish black (5 G 2/1) material, and elsewhere in the unit dark basal layers are found, so color is not a reliable guide to grain size. There is a sharp boundary

between the β and γ units at 60 cm and another sharp boundary at 20 cm. So between 20 cm and 132 cm in this section there are two turbidites

Discussion: Both the sequences analyzed here bear the hallmarks of turbidite origin, and that in 387-27-1 contains two turbidites, a fact which was not wholly expected. The sharp boundary at 60 cm in Core 27, Section 1 is overlain by only diffusely laminated mudstone with virtually the same grain size as the sediment below, but as is seen in Figure 8, the coarse mode shift is quite distinct.

Site 386, Unit 3A (Figure 9)

A number of sand layers which appear to be of turbidite origin occur in this unit. Overlying these sands is marly nanno ooze and nanno ooze which may be part of the turbidite or may not. The sequence analyzed from Core 4, Section 5 does not shed much light on the problem. The basal sand layer is obviously different from the others; the two samples in the middle, at 103 and 77 cm, are very similar and show no evidence of
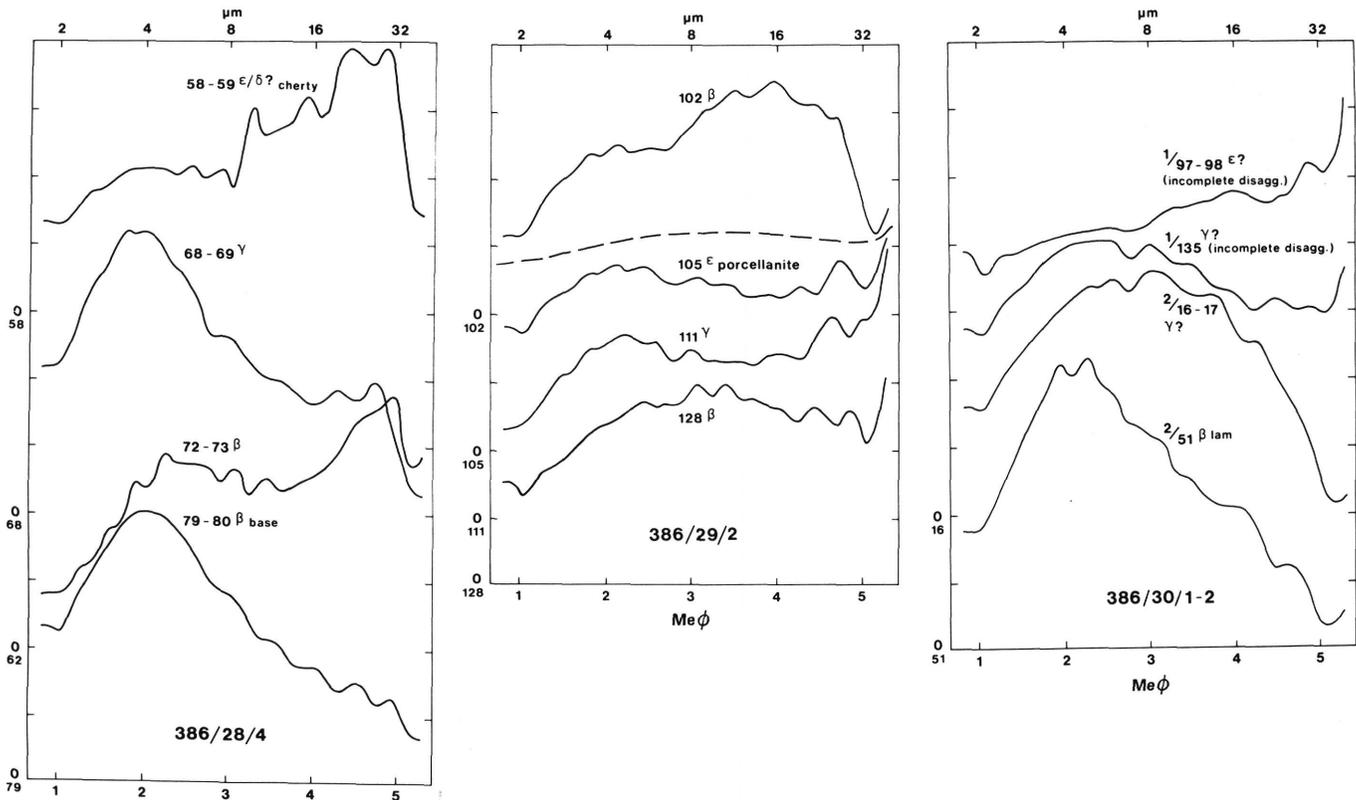
Figure 6. *Analyses of samples from Unit 4C, Site 386. The dashed line marks the boundary at the base of a cycle.*

grading, and the top sample contains a lot of clay. In fact, the samples at 77 and 103 cm also contain a lot of clay that gave flocculation problems during processing of the three upper samples. The question of whether the fine sediment above the sands is also of turbidite origin is not answered by these data.

Site 386, Unit 6 (Figure 10)

Within the green and black mudstones of Unit 6 are many homogeneous layers with a thin zone of mud-clasts at their base. The samples in 386-44-4 are from such a layer. The sample at 71 cm is somewhat finer than that from 73 cm, while the latter appears to have some material >40 μm. The basal sample has a pronounced clay mode and only a small mode of coarse material at 4.5 to 5.1 Mcϕ. Megascopically, the sample at 76.5 cm is seen to contain fine-sand-sized mud clasts. These have been disaggregated ultrasonically so that the fine component swamps the coarse. The sequence is graded, confirming the suspicion of a turbidite origin.

The samples analyzed from 386-62-4 were not expected to show any regularity of size variation. It appears, however, that there is certainly a coarsening downwards to the sample at 126 cm. This raises the possibility that rather more units in the sequence may be graded and of possible turbidite origin than at first presumed. Certainly a number of the homogeneous units, particularly where there are mud clasts at the base, seem to be perfectly good turbidites with cryptic grading.

CONCLUSIONS

The evidence of grading in progressive shift of modal peak position and for basal erosion by fine modes in basal samples gives support to the notion that many of the cycles of $\gamma\epsilon$, $\beta\gamma\epsilon$, and $\alpha\beta\gamma\epsilon$ type in Units 4D and 3B at Sites 386 and 387 are turbidites. The position of Unit 4C both between, and laterally equivalent to, units containing turbidites suggests that it too contains turbidites and that the difficulties in sample processing in this unit should not be allowed much weight in the assessment of the origin of these units. The widespread silicification will make the obtaining of any results from these units a difficult task. The homogeneous units in the green and black claystones are probably turbidites.

The method of analysis is particularly well suited to the analysis of small samples, examination of material from thin laminae and the like, but is subject to sampling problems when a very small subsample has to be taken from a large sample. The frequency diagram form of representation is more expressive visually than cumulative curves, particularly for progressive modal shifts.

These turbidites contain very little sand sized material, probably less than two per cent as a whole. Nevertheless they are not thin like the silt turbidites of the modern Sohm and Hatteras Abyssal plains (Horn et al., 1971). Piper (1973) has described similar silt turbidites up to 55 cm thick from the Gulf of Alaska. The thickness of the turbidites at Site 386 (where some are >1 m) is partly due to the fact that the site was a
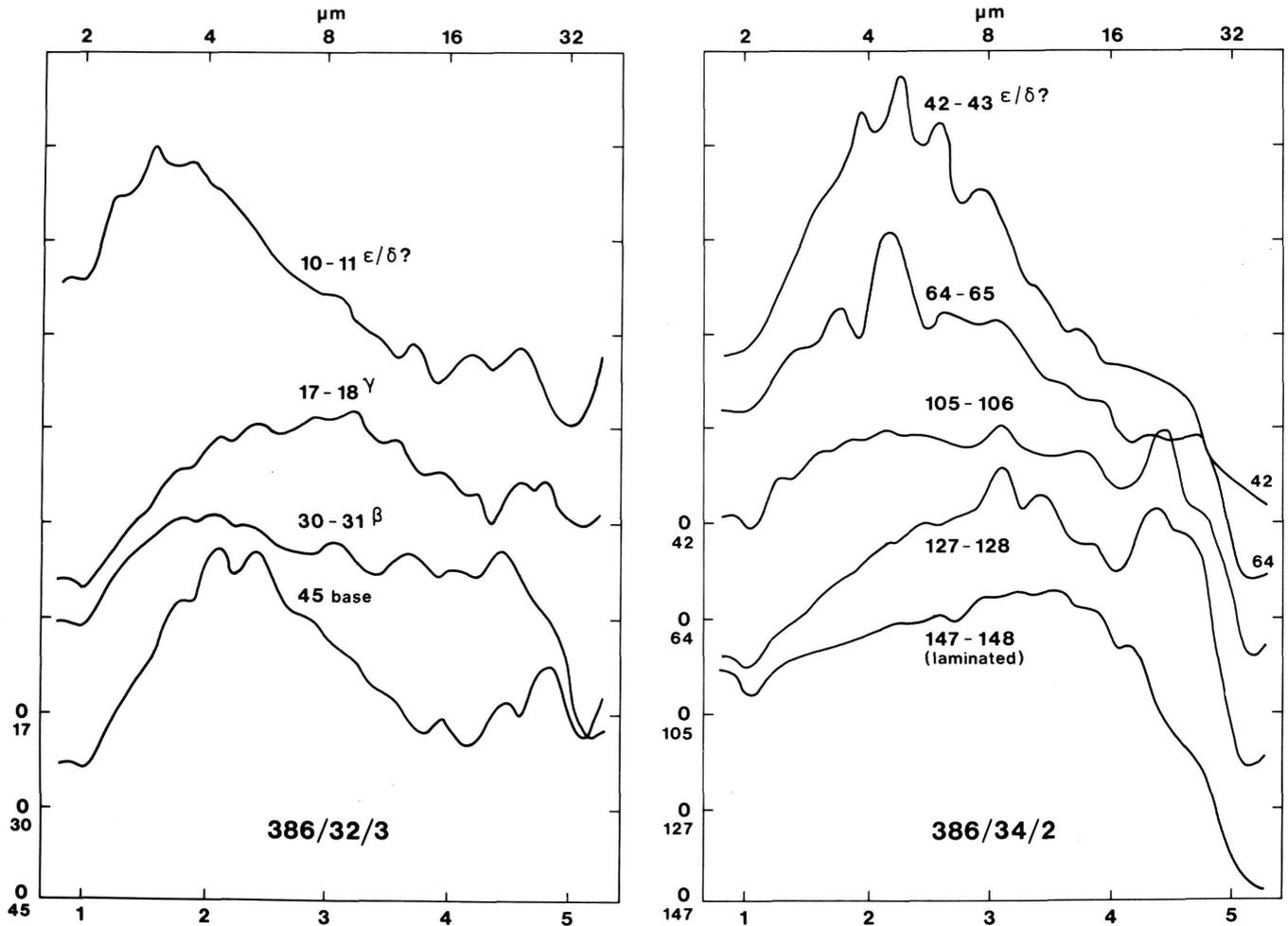
401

Figure 7. *Analyses of samples from Unit 4D, Site 386.*

sea-floor depression. Nevertheless, these units are unusual in their high silt/clay content. The dynamics of such flows are not adequately accounted for by present theories of turbidity current flow.

ACKNOWLEDGMENTS

Many thanks to my colleagues C. E. Vincent for programming the data processing and plotting routine and C. T. Baldwin for critical review of the manuscript.

REFERENCES

Bouma, A. H., 1962. *Sedimentology of some flysch deposits: A graphic approach to facies interpretation*: Amsterdam (Elsevier).

Hesse, R., 1975. Turbiditic and non-turbiditic mudstone of the Cretaceous flysch sections of the East Alps and other basins: *Sedimentology*, v. 22, p. 387-416.

Horn, D. R., Ewing, M., Horn, B. M., and Delach, M. N., 1971. Turbidites of the Hatteras and Sohm Abyssal Plains, western North Atlantic: *Marine Geol.*, v. 11, p. 287-323.

Middleton, G. V., 1967. Experiments on density and turbidity currents III. Deposition of sediment: *Canadian J. Earth Sci.*, v. 4, p. 475-505.

Piper, D. J. W., 1973. The sedimentology of silt turbidites from the Gulf of Alaska. *In* Kulm, L. D., von Huene, R., et al., *Initial Reports of the Deep Sea Drilling Project*, v. 18: Washington (U. S. Government Printing Office), p. 847-867.

Sheldon, R. P. and Parsons, T. R., 1967. *A practical manual on the use of the Coulter Counter in marine science.* Toronto (Coulter Electronics Sales Co.).

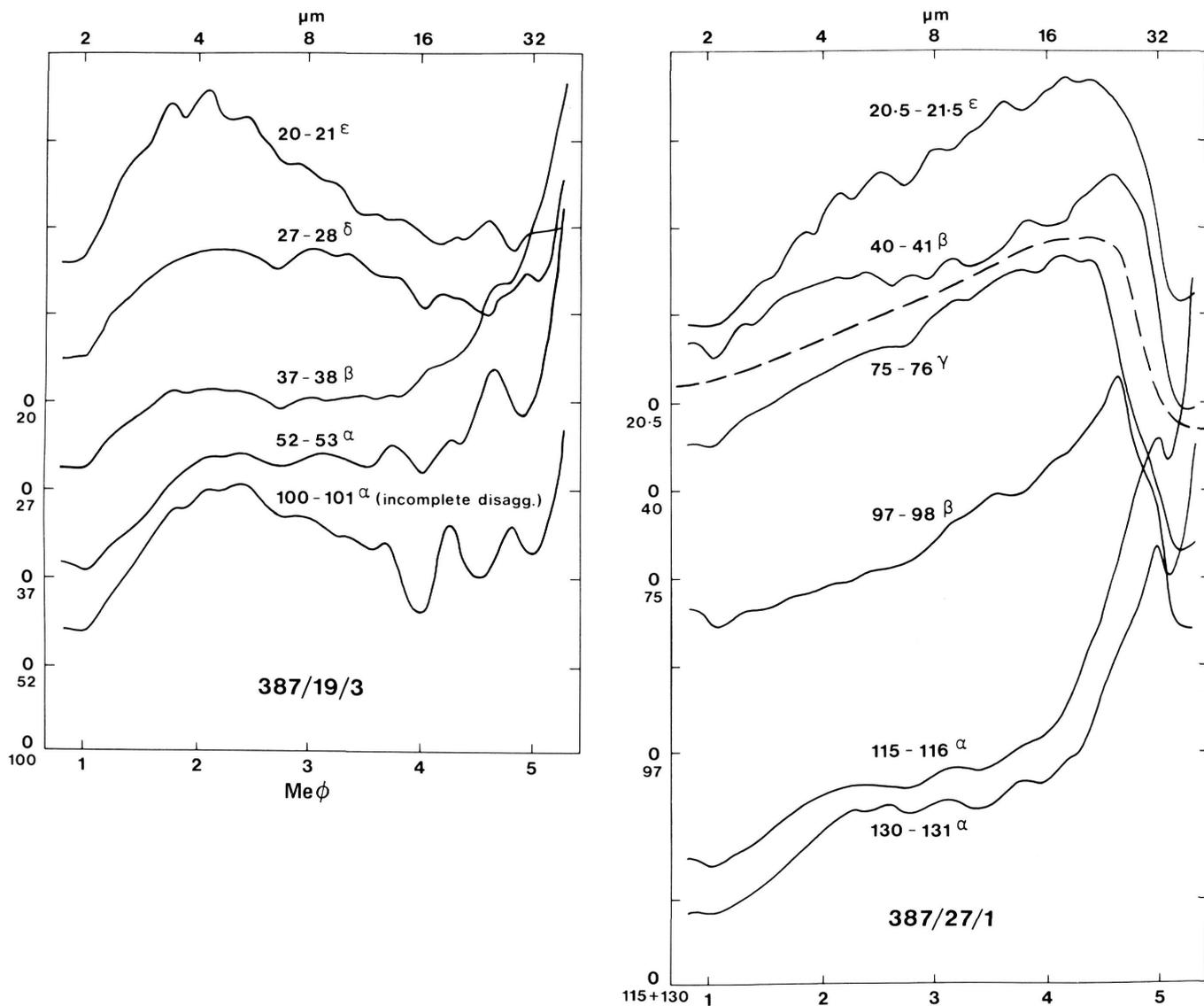Van der Lingen, G. J., 1969. The turbidite problem: *New Zealand J. Geol. Geophys.*, v. 12, p. 7-50.

Figure 8. *Analyses of samples from Unit 3B, Site 387. The dashed lin marks the boundary at the base of a cycle.*
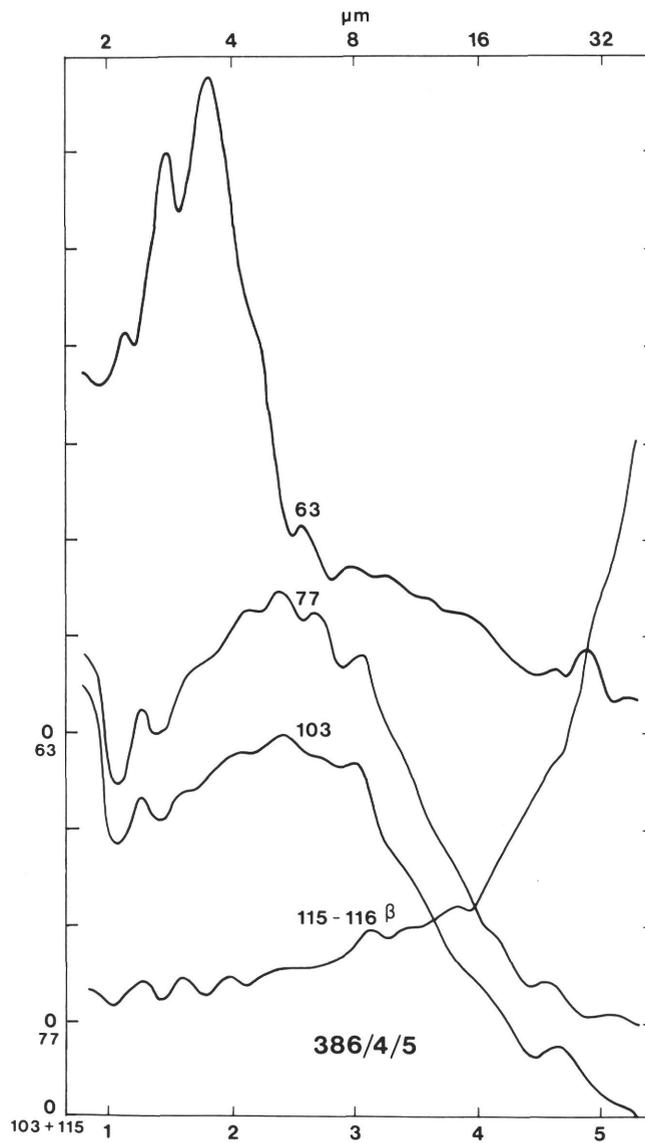
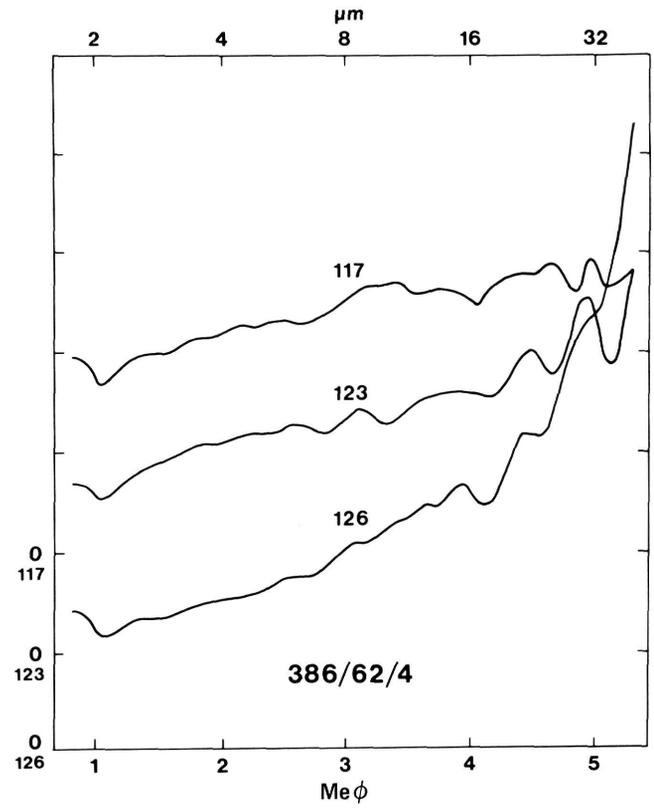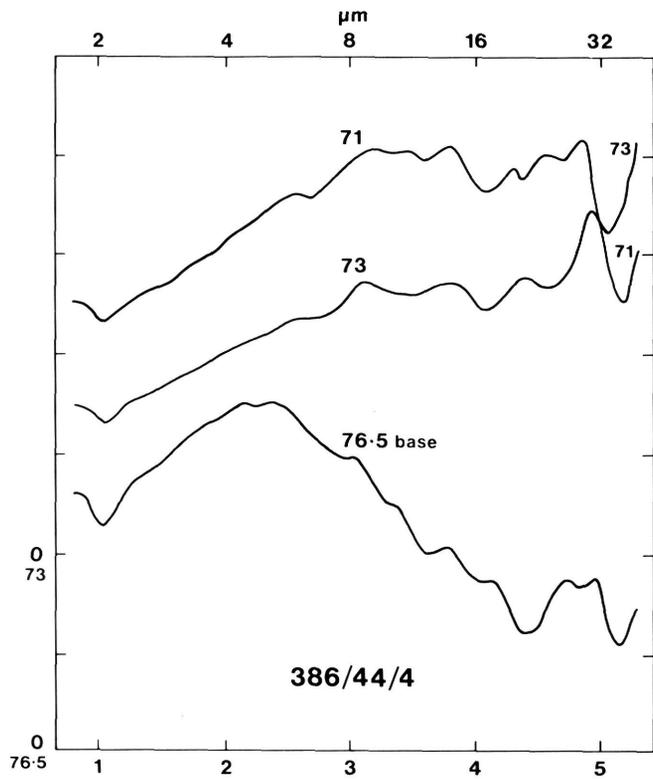Figure 9. *Analyses of samples from Unit 3A, Site 386.*

Figure 10. *Analyses of samples from Unit 6, Site 386.*